Gain and Loss of Floral Scent Production through Changes in Structural Genes during Pollinator-Mediated Speciation

Amrad, A.; Moser, M.; Mandel, T.; de Vries, M.; Schuurink, R.C.; Freitas, L.; Kuhlemeier, C.

DOI
10.1016/j.cub.2016.10.023

Publication date
2016

Document Version
Final published version

Published in
Current Biology

Article

Current Biology

Gain and Loss of Floral Scent Production through Changes in Structural Genes during Pollinator-Mediated Speciation

Highlights

- Structural genes *BSMT* and *BPBT* cause gain of scent during bee-to-moth pollination
- *CNL* was inactivated and severely degraded during moth-to-hummingbird pollination
- CNL is a target of evolutionary change across angiosperms
- Identifying functional mutations can help in the ordering of speciation events

Authors

Avichai Amrad, Michel Moser, Therese Mandel, Michel de Vries, Robert C. Schuurink, Loreta Freitas, Cris Kuhlemeier

Correspondence

cris.kuhlemeier@ips.unibe.ch

In Brief

Floral scent is an important signal for pollinators. Amrad et al. identify structural genes involved in the gain and loss of scent during shifts from bee to hawkmoth to hummingbird pollination in *Petunia*. The identification of such speciation genes provides insight into the process of speciation.

Accession Numbers

KX925198

Amrad et al., 2016, Current Biology *26*, 3303–3312
December 19, 2016
http://dx.doi.org/10.1016/j.cub.2016.10.023

CellPress

Current Biology
Article

Gain and Loss of Floral Scent Production through Changes in Structural Genes during Pollinator-Mediated Speciation

Avichai Amrad,[1] Michel Moser,[1] Therese Mandel,[1] Michel de Vries,[2] Robert C. Schuurink,[2] Loreta Freitas,[3] and Cris Kuhlemeier[1,4,*]
[1]Institute of Plant Sciences, University of Bern, Altenbergrain 21, 3013 Bern, Switzerland
[2]Swammerdam Institute for Life Sciences, University of Amsterdam, Science Park 904, 1098 XH Amsterdam, the Netherlands
[3]Laboratory of Molecular Evolution, Department of Genetics, Universidade Federal do Rio Grande do Sul, P.O. Box 15053, Avenida Bento Goncalves, 9500 Porto Alegre, Brazil
[4]Lead Contact
*Correspondence: cris.kuhlemeier@ips.unibe.ch
http://dx.doi.org/10.1016/j.cub.2016.10.023

SUMMARY

The interactions of plants with their pollinators are thought to be a driving force in the evolution of angiosperms. Adaptation to a new pollinator involves coordinated changes in multiple floral traits controlled by multiple genes. Surprisingly, such complex genetic shifts have happened numerous times during evolution. Here we report on the genetic basis of the changes in one such trait, floral scent emission, in the genus *Petunia* (Solanaceae). The increase in the quantity and complexity of the volatiles during the shift from bee to hawkmoth pollination was due to de novo expression of the genes encoding benzoic acid/salicylic acid carboxyl methyltransferase (BSMT) and benzoyl-CoA:benzyl-alcohol/2-phenylethanol benzoyltransferase (BPBT) together with moderately increased transcript levels for most enzymes of the phenylpropanoid/benzenoid pathway. Loss of cinnamate-CoA ligase (CNL) function as well as a reduction in the expression of the MYB transcription factor *ODO1* explain the loss of scent during the transition from moth to hummingbird pollination. The *CNL* gene in the hummingbird-adapted species is inactive due to a stop codon, but also appears to have undergone further degradation over time. Therefore, we propose that loss of scent happened relatively early in the transition toward hummingbird pollination, and probably preceded the loss of UV-absorbing flavonols. The discovery that CNL is also involved in the loss of scent during the transition from outcrossing to selfing in *Capsella* (Brassicaceae) (see the accompanying paper) raises interesting questions about the possible causes of deep evolutionary conservation of the targets of evolutionary change.

INTRODUCTION

Plants adapt to changes in pollinator availability by the evolution of new combinations of floral traits that can lead to reproductive isolation and ultimately speciation. Shifts in floral pollination syndromes have happened repeatedly in many taxa and are thought to be responsible for the rapid diversification of the angiosperms [1–5]. The genetic basis of shifts in pollinator attraction is likely to be complex, because multiple traits that are controlled by different genes must be involved. QTL mapping studies have identified loci of major phenotypic effect [6–14], but in most cases the identity of the genes is unknown. The best-studied trait in this respect is floral pigmentation, in large part because of the wealth of information about the biosynthetic pathways that has eased gene discovery [15–19]. In *Petunia*, at least five independent inactivations of the R2R3 MYB transcription factor AN2 are responsible for the loss of floral color during the transition from bee to moth pollination [20, 21], suggesting that the number of genes available for modification of floral traits is limited.

Floral scent is another important signal between plants and pollinators [9, 22–26], but can also attract or deter antagonists [25, 27–31]. Therefore, scent is subject to different selective pressures [9, 32–37]. So far, only a few genes have been associated with scent differences affecting pollinator attraction [9, 12, 38]. Here we use the genus *Petunia* (Solanaceae) to investigate the genetic basis of loss and gain of scent emission during the shifts from bee to moth and from moth to hummingbird pollination. The ancestral short-tube species *Petunia inflata* is pollinated by bees, whereas the two closely related long-tube species *Petunia axillaris* and *Petunia exserta* are adapted to pollination by nocturnal hawkmoths and hummingbirds, respectively. The main emitted volatiles derive from phenylalanine (Figure 1), the same molecule that is also the precursor of the anthocyanin pigments [39, 40]. *P. inflata* has purple, UV-reflecting flowers and emits a single volatile, benzaldehyde. *P. axillaris* flowers are white and UV absorbing, and emit a rich blend of volatiles during the night [37]. The three most abundant volatiles emitted by *P. axillaris*, benzylalcohol, methylbenzoate, and benzaldehyde, were shown to dominate the scent profile emitted by different hawkmoth-pollinated species and also to trigger a strong and innate

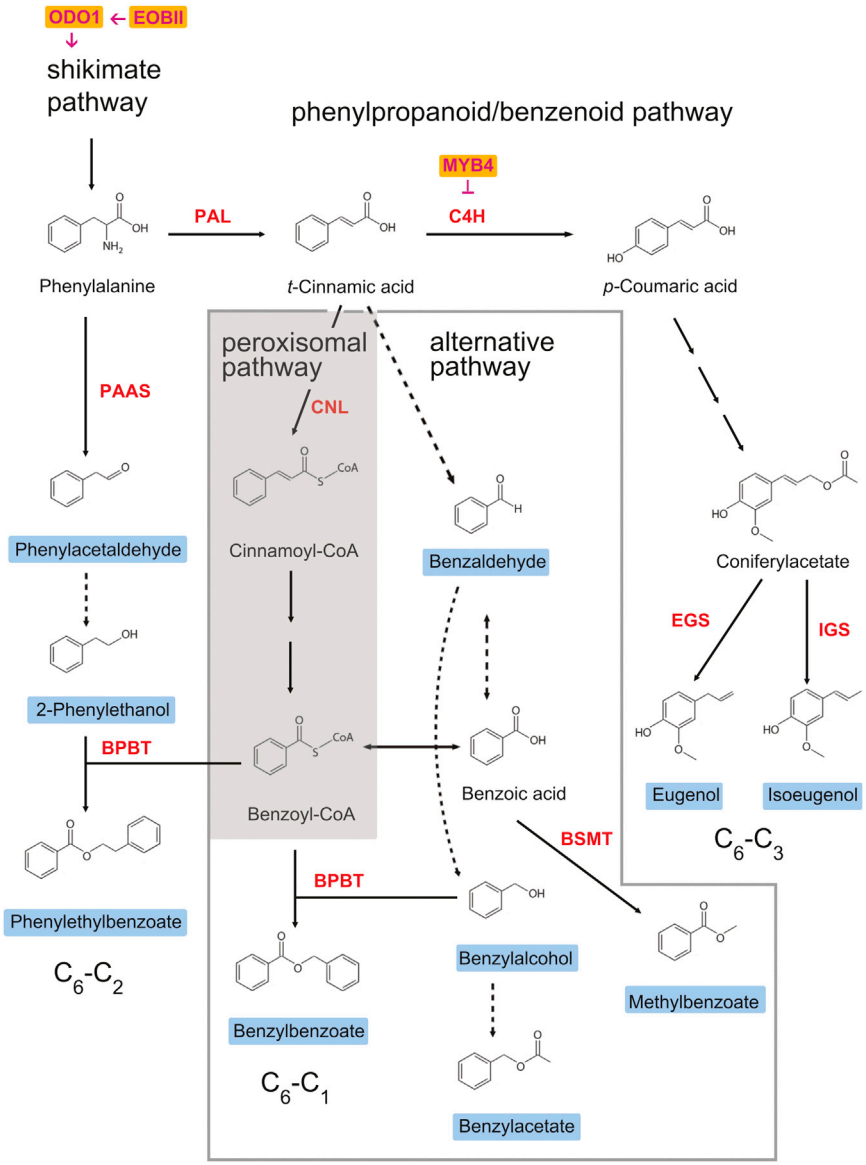

Figure 1. The Phenylpropanoid/Benzenoid Biosynthetic Pathway Leading to the Production of Volatile Compounds in *Petunia*

Volatile compounds emitted by fragrant *Petunia* are highlighted in blue. Key enzymes are shown in red. Multiple arrows simplify known enzymatic steps; steps for which enzymes/genes have not been published in *Petunia* are indicated by dashed arrows. Transcriptional regulators are highlighted in yellow. BPBT, benzoyl-CoA:benzylalcohol/2-phenylethanol benzoyltransferase; BSMT, benzoic acid/salicylic acid carboxyl methyltransferase; C4H, cinnamate 4-hydroxylase; CNL, cinnamate-CoA ligase; EGS, eugenol synthase; EOBII, emission of benzenoids II; IGS, isoeugenol synthase; ODO1, odorant1; PAAS, phenylacetaldehyde synthase; PAL, phenylalanine ammonia lyase.

response from the hawkmoth pollinator *Manduca sexta* in sensorial and behavioral assays [37, 41, 42].

Little is known about the genetics of scent production during the bee-to-hawkmoth transition. In contrast, the differences in scent emission between *P. axillaris* and *P. exserta* were previously investigated [9, 43]. Two main scent QTLs affecting pollinator attraction were identified, one on chromosome II and one on chromosome VII. Introgression of the *P. exserta* chromosome II QTL into the *P. axillaris* background abolished methylbenzoate emission, whereas introgression of the chromosome VII QTL reduced it by ~65%. Whereas the chromosome VII QTL was identified as encoding the R2R3-MYB transcription factor ODORANT1 (ODO1) [9, 44], the identity of the chromosome II QTL is unknown [9]. Interestingly, the chromosome II QTL resides in a genomic region of low recombination together with four additional QTLs [43]. The low recombination rate in this region raises interesting questions regarding the genomic architecture of pollination syndrome genes but also makes it difficult to fine-map the genes underlying these QTLs.

Here we identify *cinnamate-CoA ligase 1* (*CNL1*) as the gene on chromosome II that is responsible for the difference in scent between *P. axillaris* and *P. exserta* and show that the increase in quantity and quality of volatiles during the shift from the ancestral *P. inflata* to *P. axillaris* required activation of the genes encoding benzoic acid/salicylic acid carboxyl methyltransferase (BSMT) and benzoyl-CoA:benzylalcohol/2-phenylethanol benzoyltransferase (BPBT).

RESULTS

Mendelization of the Scent QTL on Chromosome II

In order to identify the gene(s) underlying the scent QTL on chromosome II, we constructed a near-isogenic line, IL3-2, which segregates for this genomic region in the genetic background of the *P. axillaris* parent (Figure 2A). Further backcrossing did not reveal additional breakpoints, and thus no reduction of the apparent size of the introgression. This was not unexpected, as the QTL resides in a region of suppressed recombination [43]. RNA sequencing (RNA-seq) data from the three IL3-2 genotypes, homozygous for *P. exserta* (IL3-2$^{P.exs}$) and *P. axillaris* (IL3-2$^{P.axi}$) and heterozygous (IL3-2^{het}), were compared to the *P. axillaris* genome [45]. This indicated that the three genotypes are homozygous for *P. axillaris* outside the introgressed region on chromosome II. Analysis of methylbenzoate production in the progeny of IL3-2^{het} showed that IL3-2$^{P.axi}$ and IL3-2^{het} produced high levels of methylbenzoate, whereas IL3-2$^{P.exs}$ produced none (Figure 2B). Therefore, the chromosome II QTL behaves as a single dominant Mendelian locus.

The volatiles produced by *P. axillaris* contain a benzene ring but differ in the length of the side chains (Figure 1) [46]. For a

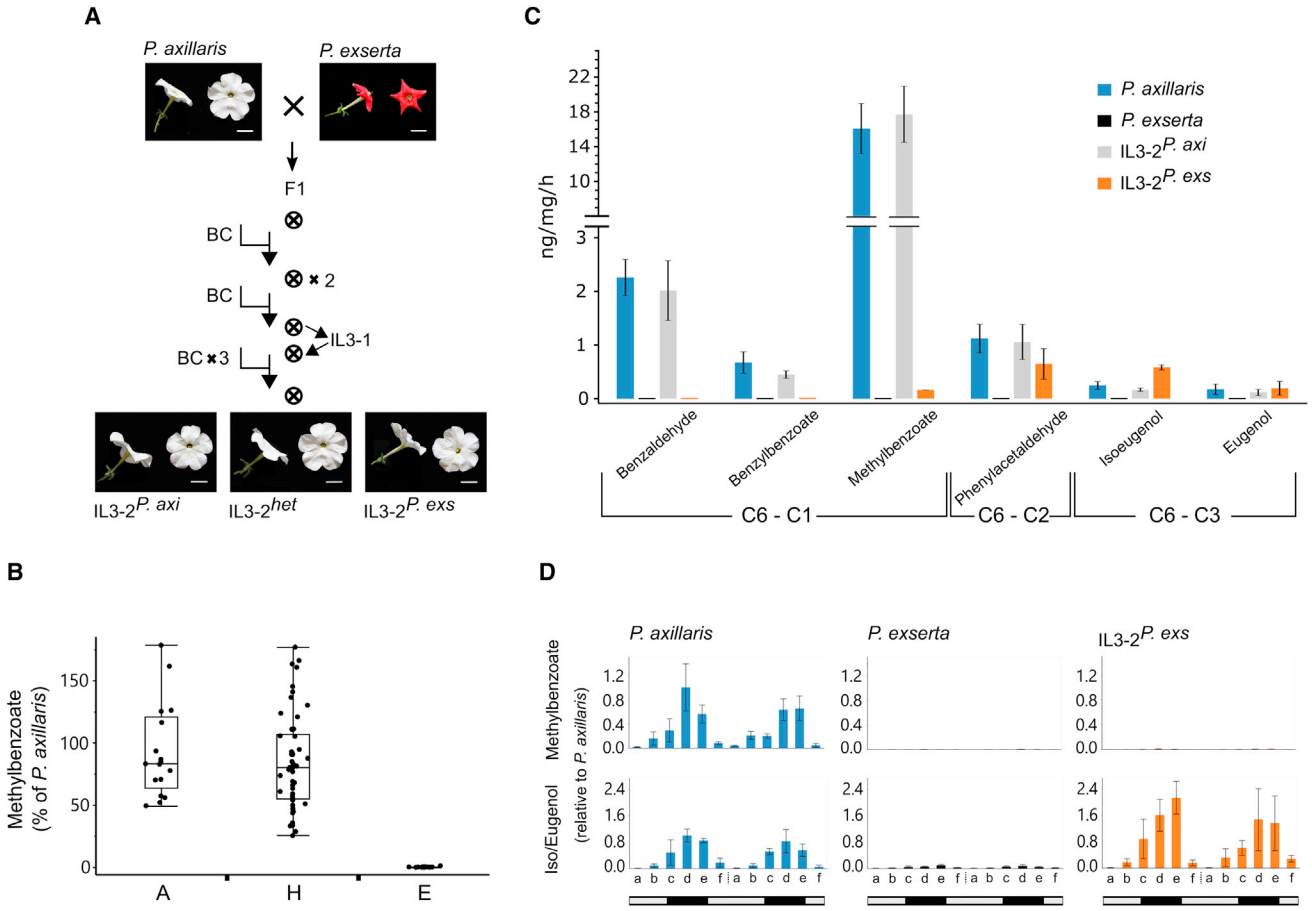

Figure 2. A Major QTL on Chromosome II Explains the Emission Difference of C_6-C_1 Compounds between *P. axillaris* and *P. exserta*

(A) Introgression line IL3-2 segregates for the chromosome II QTL in an otherwise homozygous *P. axillaris* N genetic background (see the Experimental Procedures). In total, five backcrosses (BCs) to *P. axillaris* and six self-pollinations (⊗) were done. IL3-1 was described in Hermann et al. [43]. Numbers next to symbols represent the numbers of crosses/self-pollinations. Scale bars, 2 cm.

(B) The introgressed scent trait on chromosome II shows Mendelian segregation. Methylbenzoate analysis of 93 offspring of a heterozygous IL3-2 parent scored according to chromosome II genotype: A, homozygous for the *P. axillaris* allele (n = 17); E, homozygous for the *P. exserta* allele (n = 26); H, heterozygous (n = 50). The PTR-MS result is normalized to parental *P. axillaris* values (=100%). Each box bounds the interquartile range (IQR) divided by the median, and whiskers extend to a maximum of 1.5× IQR beyond the box.

(C) The *P. exserta* chromosome II genotype has reduced scent emission of C_6-C_1 compounds. Headspace GC-MS analysis of 1-day-old open detached flowers. Volatiles were collected for 4 hr. Bars show means ± SEM; IL3-$2^{P.axi}$, n = 5; all others, n = 4.

(D) Methylbenzoate and iso/eugenol emission at 12 time points spanning 44 hr starting from a 1-day-old open flower as measured by PTR-MS on detached flowers from *P. axillaris*, *P. exserta*, and IL3-$2^{P.exs}$. Values are relative to *P. axillaris* (day 1; 19:00 hours). Bars show means ± SEM; n ≥ 3. Black and gray areas on the horizontal bar correspond to dark and light periods, respectively. Letters on the x axis represent different times of day: a, 7:00; b, 11:00; c, 15:00; d, 19:00; e, 23:00; f, 3:00.

more complete understanding of the QTL effect, we determined the floral emission of the C_6-C_1, C_6-C_2, and C_6-C_3 classes of volatiles (Figure 2C). Whereas the emission of the C_6-C_1 compounds benzaldehyde, benzylbenzoate, and methylbenzoate was severely reduced in IL3-$2^{P.exs}$ compared to IL3-$2^{P.axi}$, the emission of isoeugenol (C_6-C_3) was elevated. No measurable emission of any compound was detected in the *P. exserta* parent. This suggests that the chromosome II QTL has opposite effects on the emission of different branches of the phenylpropanoid/benzenoid pathway. It is possible that the QTL specifically affects the C_6-C_1 pathway and thereby causes metabolic flux to be redirected toward the C_6-C_3 pathway.

Iso/eugenol emission in IL3-$2^{P.exs}$ displayed a rhythmic profile, peaking during the night, similar to the methylbenzoate profile seen in *P. axillaris* (Figure 2D). Therefore, the chromosome II QTL appears not to affect the circadian rhythm of *P. axillaris*, typical for plants visited by nocturnally active pollinators [37].

Cinnamate-CoA ligase as a Candidate Gene Underlying the Chromosome II Scent QTL

To identify candidate genes underlying the QTL, we conducted an RNA-seq experiment and focused on genes encoding 18 proteins that were reliably annotated as enzymes of the shikimate, arogenate, and phenylpropanoid/benzenoid pathways, as well as five known transcription factors (Figure 3A; Table S1). Mapping

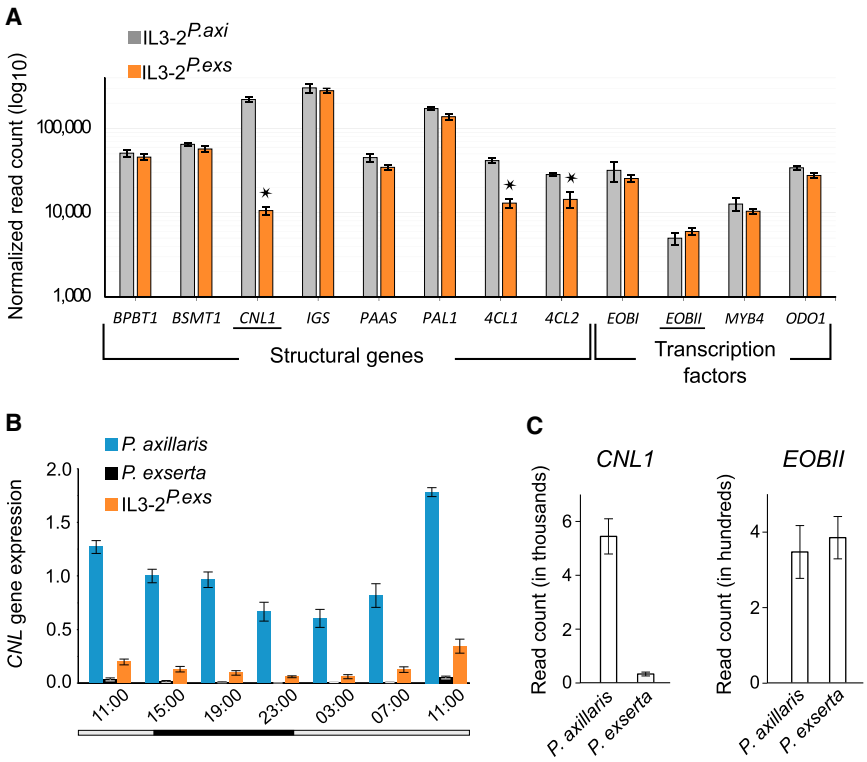

Figure 3. *CNL1* Underlies the Scent QTL on Chromosome II

(A) Gene expression profile of selected genes from the chromosome II introgression line IL3-2 in both homozygous states. Underlined genes are genes present in the chromosome II introgression. *BPBT1*, *benzoyl-CoA:benzylalcohol/2-phenylethanol benzoyltransferase*; *BSMT1*, *benzoic acid/salicylic acid carboxyl methyltransferase 1*; *CNL1*, *cinnamoyl-CoA ligase 1*; *IGS*, *isoeugenol synthase*; *PAAS*, *phenylacetaldehyde synthase*; *PAL1*, *phenylalanine ammonia lyase 1*. RNA was extracted from 1-day-old open flowers at 15:00 hours. Bars show means ± SD; n = 3. Significance-level p statistics were calculated using DESeq2 and adjusted for multiple testing with the Benjamini-Hochberg procedure to control for false discovery rate: *p < 0.001; all unmarked bars are not significantly different. For additional results for scent-related genes, see Table S1.

(B) *CNL* expression at different time points during the day/night. Transcript levels were determined by real-time qPCR analysis using universal *CNL* primers that can anneal to *CNL1*, *CNL2*, and *CNL3*. *EF1α* and *SAND* were used as reference genes; expression was normalized to that for *P. axillaris* at 15:00 hours. Bars show means ± SD; n = 3 biological replicates. Black and white areas on the horizontal bar correspond to dark and light periods, respectively.

(C) Allele-specific expression (ASE) analysis was conducted on the heterozygous IL3-2 line for the two scent-related genes that are located in the introgressed region. *CNL1* is expressed predominantly from the *P. axillaris* allele. Bars show means ± SD for reads mapped over 15 SNPs (p < 0.0001; H0, no ASE; n = 3). Both alleles of EOBII are expressed in similar amounts. Bars show means ± SD for reads mapped over 2 SNPs (p = 0.516; H0, no ASE; n = 3). Expression was measured by RNA-seq.

the SNP genotypes of the expressed genes to the *P. axillaris* genome showed that two of the three genes encoding cinnamate-CoA ligase (*CNL1* and *CNL3*) as well as the single gene encoding transcription factor EMISSION OF BENZENOIDS II (*EOBII*) reside within the introgression. Because the *EOBII* gene has no obvious functionally relevant SNPs in its coding region and was equally expressed in all genotypes, it was not further investigated. Of the *CNL* genes, only *CNL1* was expressed at an appreciable level in *P. axillaris*. Expression of *CNL1* was 20-fold lower in IL3-$2^{P.exs}$ and essentially undetectable in *P. exserta*, encouraging us to focus on this gene.

Before further discussing *CNL1*, we make the following observations. First, of the genes outside the introgression, only the two genes encoding 4-coumarate:CoA ligase (4CL) were significantly more highly expressed in IL3-$2^{P.axi}$ than in IL3-$2^{P.exs}$ (Figure 3A). These 2- to 3-fold differences in expression are statistically robust but their biological relevance may be minor, especially when considering that suppression of *4CL1* by RNAi did not affect the scent profile [47]. Second, a comparison between *P. axillaris* and IL3-$2^{P.axi}$ revealed no significant differences in expression for any of the genes, confirming that IL3-2 is highly similar to *P. axillaris* outside the introgression. Third, all genes examined except the transcription factors *EOBII* and *MYB4* were expressed at least 3-fold higher in IL3-$2^{P.exs}$ than in *P. exserta* (Table S1). This indicates the involvement of regulatory genes outside the introgression. We previously identified the transcription factor *ODO1* as the gene underlying a QTL on chromosome VII [9]. Because ODO1 is not known to regulate genes encoding enzymes involved in the final steps of the volatile phenylpropanoid/benzenoid pathway [44], we assume the influence of an additional regulatory factor, potentially underlying a QTL on chromosome III that showed an effect on the quantity, but not the composition, of compounds [9].

Loss of CNL Function Is Due to Multiple Defects within the *CNL1* Gene

qPCR analysis revealed that *CNL* is expressed in a diurnal rhythm. Expression peaks in the middle of the light period, and thus precedes peak volatile emission by approximately 8 hr. Compared to *P. axillaris*, *CNL* transcript levels were background levels in *P. exserta*. Again, we attribute the residual expression in IL3-$2^{P.exs}$ to regulatory loci outside the introgression (Figure 3B) [9].

Decreased expression can be caused by mutations in the gene itself (*cis* effects), for instance in the promoter, or by the inactivation of a regulator (*trans* effect), for instance a transcription factor. To discriminate between these two possibilities, we performed allele-specific expression (ASE) analysis in IL3-2^{het}. Expression from the *P. axillaris* allele was 16-fold higher than from the *P. exserta* allele (Figure 3C), whereas the two alleles of the *EOBII* gene, which served as a control, were equally expressed. This indicates that the difference in *CNL* expression between the two species can be attributed to a defect in the *P. exserta CNL* gene.

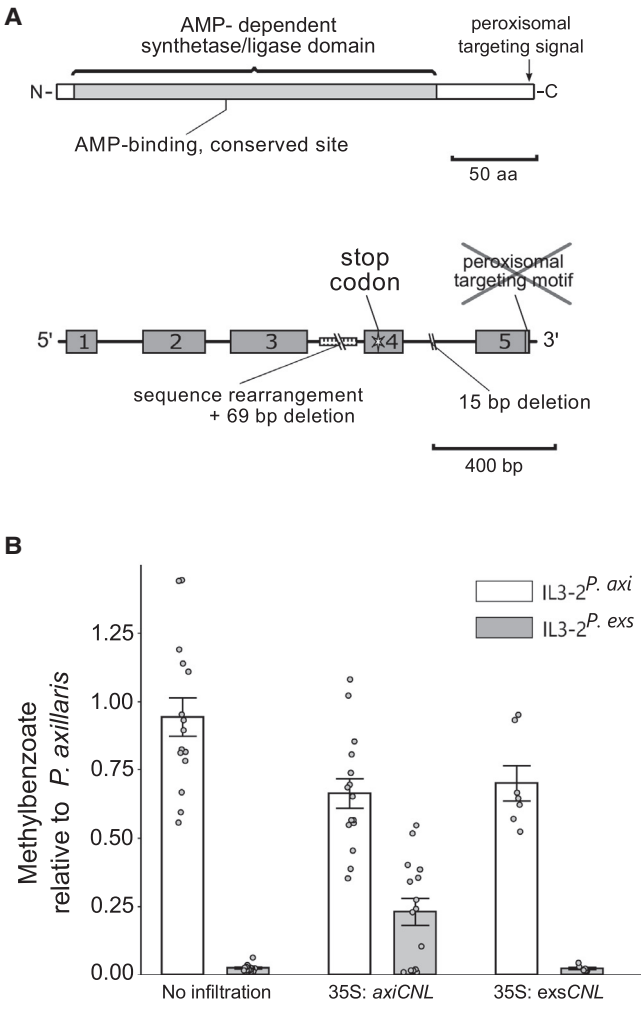

Figure 4. The *P. exserta CNL1* Coding Sequence Is Non-functional Due to a Premature Stop Codon as Well as Missense Mutations in the Peroxisomal Targeting Sequence

(A) Schematic of CNL1 protein (top). Gray boxes represent annotated conserved domains: AMP-dependent synthetase/ligase (IPR000873) and AMP-binding, conserved site (IPR020845). Schematic presentation of the *CNL1* gene sequence (bottom) indicating structural polymorphisms in the *P. exserta* copy. Gray boxes represent exons. The nonsense mutation and the missense mutations in the peroxisomal targeting sequence are indicated above the sequence.

(B) Transient expression of active *CNL1* restores methylbenzoate production. *P. axillaris* and *P. exserta CNL1* were expressed behind the 35S promoter (35S:*axiCNL* and 35S:*exsCNL*) and infiltrated into both IL3-$2^{P.axi}$ and IL3-$2^{P.exs}$ genetic backgrounds. Each data point represents a pool of four flowers. IL3-$2^{P.exs}$ 35S:*axiCNL* treatment is significantly different from 35S:*exsCNL* treatment according to non-parametric comparison for each pair using the Wilcoxon method ($p < 0.05$). Bars show means ± SEM; each of the no-infiltration and 35S:*axiCNL* treatments, n = 15; 35S:*exsCNL*, n = 6.

CNL, also known as acyl-activating enzyme, is a peroxisomal enzyme that conjugates cinnamic acid to coenzyme A, the first committed step in the C_6-C_1 pathway [47, 48]. The enzyme contains an AMP-dependent synthetase/ligase domain with a conserved AMP binding site and a peroxisomal targeting domain (Figure 4A) [47, 48]. Of the three *CNL* genes present in the *P. axillaris* genome, only *CNL1* is expressed in post-anthesis petal tissue (Table S1). The *CNL2* and *CNL3* genes are expressed at background levels and have premature stop codons creating proteins that are 42 and 196 amino acids shorter, respectively [45]. Thus, we conclude that *CNL2* and *CNL3* are pseudogenes and that *CNL1* is solely responsible for the synthesis of cinnamoyl-CoA in the peroxisomes of post-anthesis *P. axillaris* petals.

Comparing the *P. exserta* and *P. axillaris CNL1* genomic sequences reveals substantial differences likely to affect the function of the protein (Figure 4A). The protein sequence alignment reveals 22 amino acid changes, 13 of which are non-conservative. Interestingly, two out of the three amino acids making up the peroxisomal targeting signal are changed in the *P. exserta* sequence (ARL to TRI). Most striking, the *P. exserta CNL1* gene contains a nonsense mutation in the fourth exon, which is predicted to shorten the protein by 171 amino acids. This leaves the conserved AMP binding intact, but both the AMP-dependent synthetase/ligase and peroxisomal targeting domains are truncated or absent. In conclusion, the *P. exserta CNL1* gene is inactivated in at least three ways. It has severely reduced expression, encodes a truncated protein, and contains missense mutations in the peroxisomal targeting domain.

Reduction of *CNL* transcript levels by RNAi has been shown to decrease benzenoid synthesis in *Petunia hybrida* cv Mitchell [47, 48]. To confirm that it is the inactivation of *CNL1* in *P. exserta* that causes the reduction of benzenoid production in the wild *Petunia* species, we used a transient expression system to test for genetic complementation [49] (Figure 4B). As a control, constructs containing either the *P. axillaris* or *P. exserta CNL1* gene driven by the constitutive 35S promoter were infiltrated into IL3-$2^{P.axi}$ flowers. This shows that the transient assay by itself reduced methylbenzoate production by approximately 30%, probably due to the injury inflicted on the petals during the *Agrobacterium*-mediated infiltration. Most importantly, introducing the *P. axillaris CNL1* construct into IL3-$2^{P.exs}$ significantly increased methylbenzoate production, whereas the mutated *P. exserta CNL1* construct did not.

CNL1 Functional Haplotypes Differentiate between Species in Natural Populations

The presence of a nonsense codon in the *P. exserta CNL1* gene provides an opportunity to study the distribution of a causal polymorphism in natural populations. Whereas *P. exserta* is a rare species endemic to a small geographic region in Brazil, *P. axillaris* is widespread across a large area in central South America [50]. We analyzed samples from the region of sympatry, and in the case of *P. axillaris* also from multiple locations in Argentina, Uruguay, and Brazil. SNP analysis was done by sequencing an amplicon spanning the genomic location of the nonsense codon. Detailed results are presented in Table S2.

Out of 13 *P. exserta* populations, 11 populations showed exclusively the *P. exserta* genotype. One population showed both genotypes, and one population showed only the *P. axillaris* genotype. All 21 allopatric *P. axillaris* populations contained the *P. axillaris CNL1* genotype alone. In the three *P. axillaris* sympatric populations, we were able to identify one individual that showed the *P. exserta* genotype, whereas all others had the *P. axillaris* genotype. This indicates that the *P. exserta* genotype is limited

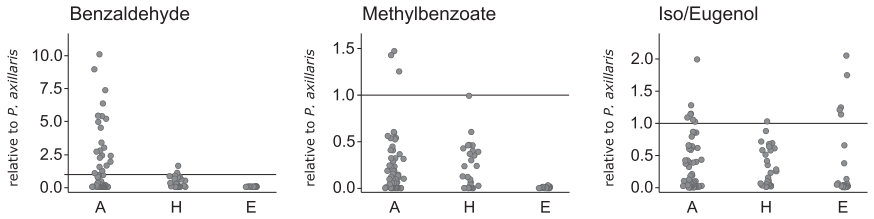

Figure 5. The *P. exserta CNL1* Genotype Correlates Perfectly with the Absence of Methylbenzoate and Benzaldehyde Production in the Putative Hybrid Line Population

From 27 plants showing intermediate morphology sampled from the Pedra da Cruz population, 112 offspring were genotyped for *CNL1* and phenotyped for scent emission by PTR-MS. A, homozygous for the *P. axillaris*-like allele; E, homozygous for the *P. exserta*-like allele; H, heterozygous. The horizontal bars represent *P. axillaris* N reference accession values. For complete phenotypic, genotypic, and germline information, see Table S3. See also Table S2.

to the *P. exserta* distribution area and most likely originated there. It suggests an advanced fixation process of the different alleles in the different species and also is in line with an ongoing process of hybridization in regions of sympatry as shown in previous studies [50, 51].

The wild germplasm genotyping enabled us to establish a connection between *CNL1* alleles and species, but the lack of phenotypic data on those samples prevented phenotype-genotype association. Therefore, we continued by examining individuals from Pedra da Cruz, a population that includes putative *P. axillaris* × *P. exserta* hybrids [50, 52]. We collected 27 seed capsules from 27 plants in the wild, and seeds from these capsules were sown and self-pollinated to produce 112 plants (Figure 5; for full progeny and phenotypic data, see Table S3). All plants homozygous for the *P. exserta* allele were devoid of methylbenzoate or benzaldehyde production. Plants homozygous for the *P. axillaris* allele or heterozygotes showed a wide spectrum of C_6-C_1 volatile production, ranging from ten times the reference accession *P. axillaris* N to no production. This shows that the *P. axillaris* CNL is absolutely required for the emission of C_6-C_1 volatiles but that it is not sufficient. Presumably, additional genetic factors segregating in the unknown genetic background of these lines, e.g., the previously described *ODO1* and QTL on chromosome III, are also required [9]. In contrast, production of the C_6-C_3 volatile iso/eugenol did not show any correlation with the *CNL1* haplotype, confirming the results obtained from the IL3-2 analysis (Figure 2C).

CNL1 Is Both Expressed and Active in *P. inflata*

The severe erosion of *P. exserta CNL1* strongly suggests that the direction of evolution was from active to inactive CNL and that *P. exserta* is a derived species. The ancestral bee-pollinated species *P. inflata* produces significant amounts of benzaldehyde but none of the other compounds emitted by *P. axillaris* [37]. This raises the question of the genetic basis of the increase in the quantity and diversity of scent emission during the evolution from the ancestral clade to *P. axillaris*. Because the sequences of *CNL* and other scent-related genes indicated no inactivations of the coding regions [45], we investigated differential expression by RNA-seq analysis. Results showed that in *P. axillaris*, the expression of most genes, including *CNL1*, is moderately higher than in *P. inflata* (Table S4). This is consistent with the net increase of phenylpropanoids/benzenoids in *P. axillaris*.

Special cases are *BPBT* encoding the enzyme benzoyl-CoA: benzylalcohol/2-phenylethanol benzoyltransferase and the two copies of *BSMT* encoding benzoic acid/salicylic acid carboxyl methyltransferase, which are not expressed at all in *P. inflata* (Figure 6A). Furthermore, analysis done on *P. inflata* × *P. axillaris* F1 hybrids showed that for these three genes only the *P. axillaris* alleles are expressed in the F1, indicating that the difference in expression is caused by *cis*-acting polymorphisms (Figure 6B). BSMT is responsible for the last step in methylbenzoate synthesis in *Petunia* [53], and therefore the absence of *BSMT* mRNA in *P. inflata* provides a sound explanation for the lack of methylbenzoate production. *BPBT* is responsible for the synthesis of benzylbenzoate and phenylethylbenzoate from benzoyl-CoA and benzyl alcohol or 2-phenylethanol, respectively [54]. Downregulation of *BPBT* in *P. hybrida* plants resulted in elimination of benzylbenzoate and phenylethylbenzoate formation but also reduction of methylbenzoate emission and increased emission of benzyl alcohol and benzaldehyde [55]. Therefore, activation of BSMT and BPBT in *P. axillaris* could redirect metabolic flux away from benzaldehyde toward methylbenzoate as well as toward the additional volatiles emitted by *P. axillaris*.

To provide genetic support for the transcriptome results, we performed a double-complementation test by crossing *P. inflata* and *P. exserta*, which both lack methylbenzoate. *P. exserta* contains an active *BSMT* copy but inactive *CNL1* and *ODO1* copies whereas, conversely, *P. inflata* has an inactive *BSMT* but active *CNL1* and *ODO1* copies. Therefore, the F1 will be heterozygous for active copies of all three genes. The GC-MS results clearly show that methylbenzoate production is restored in the F1, confirming complementation (Figure 6C). Note, however, that methylbenzoate is produced in the F1 at around 10% of the level in *P. axillaris* (Figures 2C and 6C). Full complementation to *P. axillaris* levels must therefore require additional components that are present in *P. axillaris* but neither in *P. inflata* nor in *P. exserta*. The reduced volatile emission may be attributed to reduced levels of active *ODO1*, *CNL1*, and *BSMT* transcripts as well as additional unidentified factors, e.g., the QTL on chromosome III [9].

DISCUSSION

In this work, we have shown that the increase in volatile emission during the shift from ancestral bee pollination to the hawkmoth pollination syndrome involved *cis*-acting mutations that turn on BSMT and BPBT expression. Moreover, moderate upregulation of most structural genes in *P. axillaris*, most likely by an unknown transcription factor, appears to be responsible for the increase in the overall amount of volatiles. Therefore, the gain of function proceeded through mutations in *cis*-acting and transacting regulatory mutations in a preexisting pathway.

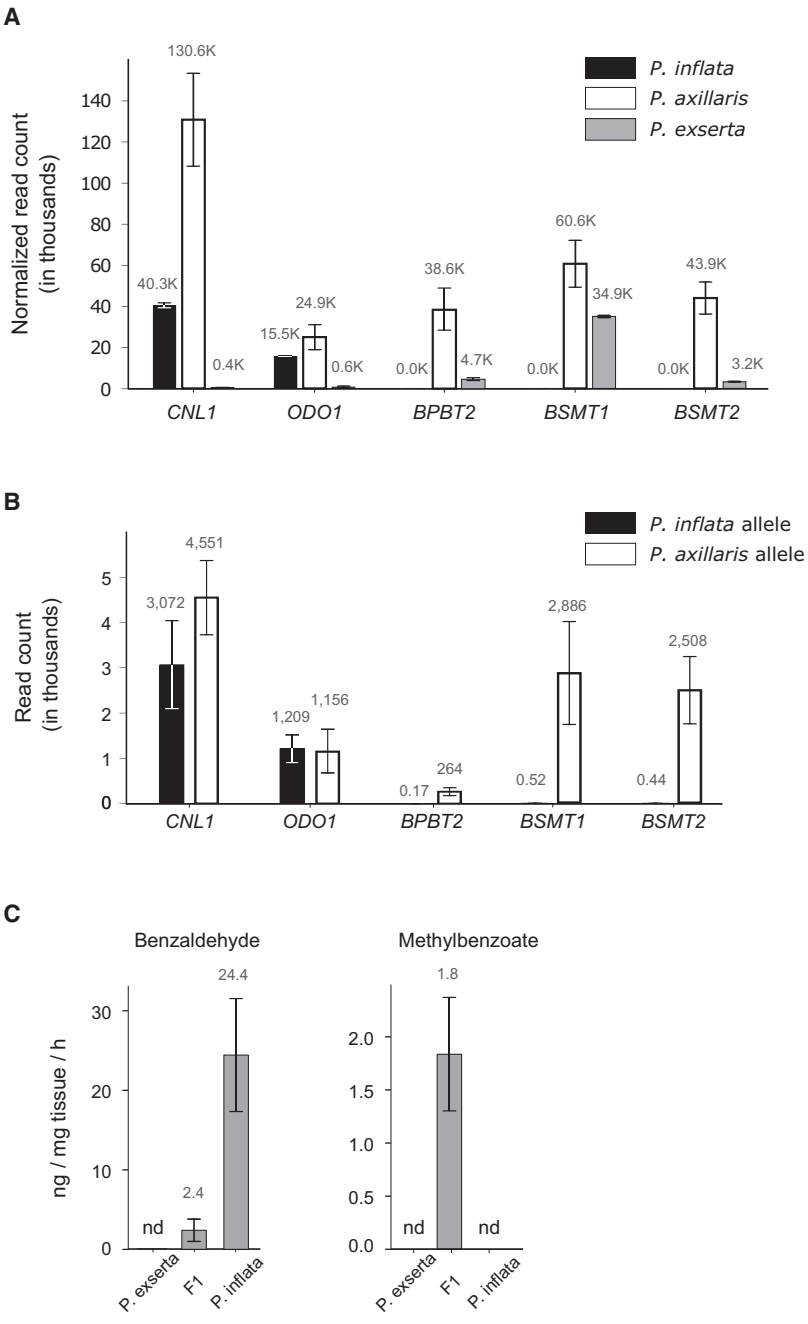

Figure 6. Differential Expression of Structural Genes Explains the Difference in Scent Emission between Bee-Pollinated *P. inflata* and Hawkmoth-Pollinated *P. axillaris*

(A) RNA-seq analysis shows moderate upregulation of *CNL* and *ODO1* and de novo expression of *BPBT2* and *BSMT* in *P. axillaris* compared to *P. inflata*. Note that *BSMT* and *BPBT2* are expressed in non-scented *P. exserta*, but not in *P. inflata*. Significance-level p statistics were calculated using DESeq2 and adjusted for multiple testing with the Benjamini-Hochberg procedure to control for false discovery rate. All gene expression differences between the species are significantly different, $p < 0.001$, except the difference between *P. axillaris* and *P. exserta BSMT1*, $p < 0.01$, and the difference between *P. axillaris* and *P. inflata ODO1*, which is not significant. Bars show means ± SD; n = 3. For additional results for scent-related genes, see Table S4.

(B) *cis*-acting mutations downregulate *BSMT* and *BPBT* in *P. inflata*. ASE analysis was conducted on the F1 from a cross between *P. axillaris* and *P. inflata*. *BSMT1*, *BSMT2*, and *BPBT2* are expressed predominantly from the *P. axillaris* allele. Bars show means ± SD for reads mapped over 8, 9, 3, 14, and 11 SNPs in *BPBT2*, *BSMT1*, *BSMT2*, *CNL1*, and *ODO1*, respectively. For *CNL1*, *BPBT2*, *BSMT1*, and *BSMT2*, expression was significantly higher for the *P. axillaris* allele ($p < 0.0001$; H0, no ASE; n = 3); *ODO1* showed no significant ASE ($p = 0.52$; H0, no ASE; n = 3). Expression was measured by RNA-seq.

(C) Complementation test for methylbenzoate production in F1 from a cross between *P. exserta* and *P. inflata*. GC-MS volatile analysis of a 1-day-old open detached flower. Volatiles were collected for 4 hr. Bars show means ± SEM; n = 3. nd, not detected.

Functional inactivation in *CNL1* underlies the QTL on chromosome II and, together with the previously identified MYB transcription factor ODO1 [9], accounts for the loss of scent during the shift from hawkmoth to hummingbird pollination syndrome. During this transition, CNL1 was inactivated in three ways: the transcription of the gene is reduced to background levels, the peroxisomal targeting sequence is inactivated, and a stop codon deletes the C-terminal part of the protein. The stop codon is present in all but one of the *P. exserta* populations, and would by itself probably suffice to obliterate gene function. Whatever the primary inactivating event, it appears that the gene has degenerated subsequent to losing its functionality. The severe degeneration of *CNL1* is in stark contrast to *MYB-FL*, the gene responsible for the loss of UV-absorbing flavonols in *P. exserta* [52]. MYB-FL also sustained a nonsense mutation but appears to encode an otherwise functionally intact protein and is expressed at the RNA level. This suggests that *MYB-FL* inactivation is a more recent event that happened after the inactivation of *CNL1*. We have previously argued that, due to metabolic competition, it is unlikely that *P. exserta* re-acquired its intense red color in the presence of MYB-FL [52]. Therefore, we tentatively order the steps in the shift of advertising floral traits as (1) loss of scent, (2) loss of flavonols, and (3) gain of visible color.

CNL1 presents yet another case of a change in a single gene that has a major effect on pollinator preference [9]. This leads to one of the key questions in evolutionary biology, namely whether such large-effect mutations are rare exceptions possible only in specialized pathways of secondary metabolism, or whether they are a common response to strong selection pressure [56–58]. A related question is: why *CNL1* was selected as a target of evolutionary change rather than one of the other structural and regulatory genes in the pathway? An obvious answer

is that *CNL* catalyzes the first committed step of the C_6-C_1 pathway, and therefore loss of *CNL* function abolishes the production of the volatiles that are key attractants of the hawkmoth pollinator *M. sexta* [35, 37, 59]. Absence of scent is unlikely to help attract hummingbirds but may reduce metabolic costs for *P. exserta*, which grows in a shaded, N-rich environment and therefore is probably carbon limited. Perhaps more important, volatiles are "open communication channels" that also attract unwanted visitors such as herbivores [29–31, 60]. If this idea is correct, exposing the two introgression lines IL3-2^{PaxN} (*Petunia axillaris N*) and IL3-$2^{P.exs}$ to the herbivore community in the natural environment of *P. exserta* should show more herbivory on the scented than on the unscented line. Alternatively, it could be that *CNL* loss caused the least collateral damage.

Loss of floral color during the transition from bee to hawkmoth pollination involved loss of function in AN2, presumably because AN2's only known function is to induce the expression of the terminal enzymes of the anthocyanin biosynthetic pathway [20, 21]. The topology of the phenylpropanoid/benzenoid biosynthetic pathway is more complex than anthocyanin biosynthesis, and may allow even fewer opportunities for major change without unwanted side effects. Modification of transcription factors that have been proposed as preferred evolutionary targets [61] may also be problematic in this case due to the complex interactions of presently known genes [44, 62–64]. The finding that the loss of floral scent during the transition from outcrossing to selfing in the genus *Capsella* was also caused by loss of *CNL* function suggests that *CNL* may be a preferred target across the angiosperms (see the accompanying paper by Sas et al. [65]), giving us a remarkable example of parallel evolution identified at the molecular level.

EXPERIMENTAL PROCEDURES

All wild and laboratory accessions are described by Sheehan et al. [52]. Complete marker and mapping information for IL3-1 can be found in Hermann et al. [43]. Cleaved amplified polymorphic sequence (CAPS) markers EOBII, LO2-O2, cn9140, and ODO1 were used in the breeding process (http://www.botany.unibe.ch/deve/caps/index.html). Plants were grown in growth chambers as described by Klahre et al. [9]. Genotyping and marker regression analysis details can be found in the Supplemental Experimental Procedures.

Proton transfer reaction mass spectroscopy (PTR-MS) data collection was done as described by Klahre et al. [9]. MS does not separate eugenol and isoeugenol, and therefore they were analyzed as a single compound. For volatile measurement in the transient expression analysis experiment, see the Supplemental Experimental Procedures.

For volatile headspace analysis, we used flowers 1 day after anthesis that were harvested 1 hr before dark. Volatile collection was done for 4 hr essentially as described by Verdonk et al. [44]. The GC-MS protocol was as described by Shaipulah et al. [66].

For qRT-PCR analysis and RNA-seq, flower limb samples were collected 1 day after anthesis at 15:00 hours. Detailed experimental procedures for qRT-PCR, RNA-seq, and ASE analysis can be found in the Supplemental Experimental Procedures.

Constructs for transient expression analysis were assembled with Gibson Assembly mix (New England Biolabs). The *CNL* coding regions, cauliflower mosaic virus (CaMV) 35S promoter, and the vector pGreenII were PCR amplified, and fragments were assembled according to the manufacturer's recommendations. Vectors were introduced into *Agrobacterium tumefaciens* strain GV3101. For transformation assays and volatile analysis, see the Supplemental Experimental Procedures.

All RNA-seq data have been deposited in the NCBI Sequence Read Archive under BioProjects SRA: PRJNA344710 and PRJNA344560. All *P. axillaris* and *P. inflata* gene sequences are available on the Sol Genomics Network at https://solgenomics.net with the annotation numbers provided in Table S1. *P. exserta CNL1* gene sequences are GenBank: KX925198. All primer details are in the Supplemental Experimental Procedures.

ACCESSION NUMBERS

The accession numbers for the RNA-seq data and *P. exserta CNL1* gene sequences reported in this paper are NCBI SRA: PRJNA344710 and PRJNA344560 and GenBank: KX925198, respectively.

SUPPLEMENTAL INFORMATION

Supplemental Information includes Supplemental Experimental Procedures and four tables and can be found with this article online at http://dx.doi.org/10.1016/j.cub.2016.10.023.

AUTHOR CONTRIBUTIONS

A.A. and C.K. conceived the project and wrote the manuscript. A.A., M.M., T.M., M.d.V., R.C.S., and L.F. designed and performed experiments and commented on the manuscript.

ACKNOWLEDGMENTS

We thank Christopher Ball, Jasmin Sekulovski, and Raphaela Lüdi for expert care of our plants; Moritz Saxenhofer, Anna Feller, and Christoph Zwahlen for help with genotyping and phenotyping; Ana Lucia Segatto and Caroline Turchetto for field collection and DNA extraction; Korinna Esfeld, Hester Sheehan, and Sarah Robinson for comments on the manuscript; Korinna Esfeld, Hester Sheehan, Daniele Roppolo, Oz Barazani, Mathieu Hanemian, and Natalia Dudareva for advice and suggestions throughout the project; Claudia Sas and Alon Cna'ani for help with the transient expression assay; Pierre Barbier de Reuille for statistical advice; and Roman Köpfli and Naama Rona Amrad for assistance with figures. We gratefully acknowledge financial support from the Swiss National Science Foundation (17-429), SystemX.ch (36-792), and the University of Bern.

Received: August 18, 2016
Revised: October 6, 2016
Accepted: October 12, 2016
Published: December 1, 2016

REFERENCES

1. Mitchell, R.J., Irwin, R.E., Flanagan, R.J., and Karron, J.D. (2009). Ecology and evolution of plant-pollinator interactions. Ann. Bot. (Lond.) *103*, 1355–1363.
2. Grant, V. (1949). Pollination systems as isolating mechanisms in angiosperms. Evolution *3*, 82–97.
3. Fenster, C.B., Armbruster, W.S., Wilson, P., Dudash, M.R., and Thomson, J.D. (2004). Pollination syndromes and floral specialization. Annu. Rev. Ecol. Evol. Syst. *35*, 375–403.
4. Knapp, S. (2010). On 'various contrivances': pollination, phylogeny and flower form in the Solanaceae. Philos. Trans. R. Soc. Lond. B Biol. Sci. *365*, 449–460.
5. Whittall, J.B., and Hodges, S.A. (2007). Pollinator shifts drive increasingly long nectar spurs in columbine flowers. Nature *447*, 706–709.
6. Bradshaw, H.D., Jr., Otto, K.G., Frewen, B.E., McKay, J.K., and Schemske, D.W. (1998). Quantitative trait loci affecting differences in floral morphology between two species of monkeyflower (*Mimulus*). Genetics *149*, 367–382.
7. Bradshaw, H.D., Jr., and Schemske, D.W. (2003). Allele substitution at a flower colour locus produces a pollinator shift in monkeyflowers. Nature *426*, 176–178.

8. Bouck, A., Wessler, S.R., and Arnold, M.L. (2007). QTL analysis of floral traits in Louisiana iris hybrids. Evolution *61*, 2308–2319.
9. Klahre, U., Gurba, A., Hermann, K., Saxenhofer, M., Bossolini, E., Guerin, P.M., and Kuhlemeier, C. (2011). Pollinator choice in *Petunia* depends on two major genetic loci for floral scent production. Curr. Biol. *21*, 730–739.
10. Brothers, A.N., Barb, J.G., Ballerini, E.S., Drury, D.W., Knapp, S.J., and Arnold, M.L. (2013). Genetic architecture of floral traits in *Iris hexagona* and *Iris fulva*. J. Hered. *104*, 853–861.
11. Wessinger, C.A., Hileman, L.C., and Rausher, M.D. (2014). Identification of major quantitative trait loci underlying floral pollination syndrome divergence in *Penstemon*. Philos. Trans. R. Soc. Lond. B Biol. Sci. *369*, 20130349.
12. Byers, K.J.R.P., Vela, J.P., Peng, F., Riffell, J.A., and Bradshaw, H.D., Jr. (2014). Floral volatile alleles can contribute to pollinator-mediated reproductive isolation in monkeyflowers (*Mimulus*). Plant J. *80*, 1031–1042.
13. Bradshaw, H.D., Jr., Wilbert, S.M., Otto, K.G., and Schemske, D.W. (1995). Genetic mapping of floral traits associated with reproductive isolation in monkeyflowers (*Mimulus*). Nature *376*, 762–765.
14. Nakazato, T., Rieseberg, L.H., and Wood, T.E. (2013). The genetic basis of speciation in the *Giliopsis* lineage of *Ipomopsis* (Polemoniaceae). Heredity (Edinb) *111*, 227–237.
15. Yuan, Y.-W., Sagawa, J.M., Young, R.C., Christensen, B.J., and Bradshaw, H.D., Jr. (2013). Genetic dissection of a major anthocyanin QTL contributing to pollinator-mediated reproductive isolation between sister species of *Mimulus*. Genetics *194*, 255–263.
16. Hopkins, R., and Rausher, M.D. (2011). Identification of two genes causing reinforcement in the Texas wildflower *Phlox drummondii*. Nature *469*, 411–414.
17. Hopkins, R., and Rausher, M.D. (2012). Pollinator-mediated selection on flower color allele drives reinforcement. Science *335*, 1090–1092.
18. Des Marais, D.L., and Rausher, M.D. (2010). Parallel evolution at multiple levels in the origin of hummingbird pollinated flowers in *Ipomoea*. Evolution *64*, 2044–2054.
19. Schwinn, K., Venail, J., Shang, Y., Mackay, S., Alm, V., Butelli, E., Oyama, R., Bailey, P., Davies, K., and Martin, C. (2006). A small family of *MYB*-regulatory genes controls floral pigmentation intensity and patterning in the genus *Antirrhinum*. Plant Cell *18*, 831–851.
20. Quattrocchio, F., Wing, J., van der Woude, K., Souer, E., de Vetten, N., Mol, J., and Koes, R. (1999). Molecular analysis of the *anthocyanin2* gene of *Petunia* and its role in the evolution of flower color. Plant Cell *11*, 1433–1444.
21. Hoballah, M.E., Gübitz, T., Stuurman, J., Broger, L., Barone, M., Mandel, T., Dell'Olivo, A., Arnold, M., and Kuhlemeier, C. (2007). Single gene-mediated shift in pollinator attraction in *Petunia*. Plant Cell *19*, 779–790.
22. Kessler, D., Kallenbach, M., Diezel, C., Rothe, E., Murdock, M., and Baldwin, I.T. (2015). How scent and nectar influence floral antagonists and mutualists. eLife *4*, e07641.
23. Dötterl, S., Jürgens, A., Seifert, K., Laube, T., Weissbecker, B., and Schütz, S. (2006). Nursery pollination by a moth in *Silene latifolia*: the role of odours in eliciting antennal and behavioural responses. New Phytol. *169*, 707–718.
24. Schiestl, F.P., Ayasse, M., Paulus, H.F., Löfstedt, C., Hansson, B.S., Ibarra, F., and Francke, W. (1999). Orchid pollination by sexual swindle. Nature *399*, 421.
25. Byers, K.J.R.P., Bradshaw, H.D., Jr., and Riffell, J.A. (2014). Three floral volatiles contribute to differential pollinator attraction in monkeyflowers (*Mimulus*). J. Exp. Biol. *217*, 614–623.
26. Chen, C., Song, Q., Proffit, M., Bessière, J.-M., Li, Z., and Hossaert-McKey, M. (2009). Private channel: a single unusual compound assures specific pollinator attraction in *Ficus semicordata*. Funct. Ecol. *23*, 941–950.
27. Schiestl, F.P., Kirk, H., Bigler, L., Cozzolino, S., and Desurmont, G.A. (2014). Herbivory and floral signaling: phenotypic plasticity and tradeoffs between reproduction and indirect defense. New Phytol. *203*, 257–266.
28. Willmer, P.G., Nuttman, C.V., Raine, N.E., Stone, G.N., Pattrick, J.G., Henson, K., Stillman, P., McIlroy, L., Potts, S.G., and Knudsen, J.T. (2009). Floral volatiles controlling ant behaviour. Funct. Ecol. *23*, 888–900.
29. Junker, R.R., and Blüthgen, N. (2010). Floral scents repel facultative flower visitors, but attract obligate ones. Ann. Bot. (Lond.) *105*, 777–782.
30. Kessler, D., Diezel, C., Clark, D.G., Colquhoun, T.A., and Baldwin, I.T. (2013). *Petunia* flowers solve the defence/apparency dilemma of pollinator attraction by deploying complex floral blends. Ecol. Lett. *16*, 299–306.
31. Theis, N., and Adler, L.S. (2012). Advertising to the enemy: enhanced floral fragrance increases beetle attraction and reduces plant reproduction. Ecology *93*, 430–435.
32. Gregg, K.B. (1983). Variation in floral fragrances and morphology: incipient speciation in Cycnoches? Bot. Gaz. *144*, 566–576.
33. Knudsen, J.T. (1994). Floral scent variation in the *Pyrola rotundifolia* complex in Scandinavia and western Greenland. Nord. J. Bot. *14*, 277–282.
34. Raguso, R.A., Levin, R.A., Foose, S.E., Holmberg, M.W., and McDade, L.A. (2003). Fragrance chemistry, nocturnal rhythms and pollination "syndromes" in *Nicotiana*. Phytochemistry *63*, 265–284.
35. Levin, R.A., Raguso, R.A., and McDade, L.A. (2001). Fragrance chemistry and pollinator affinities in Nyctaginaceae. Phytochemistry *58*, 429–440.
36. Waelti, M.O., Muhlemann, J.K., Widmer, A., and Schiestl, F.P. (2008). Floral odour and reproductive isolation in two species of *Silene*. J. Evol. Biol. *21*, 111–121.
37. Hoballah, M.E., Stuurman, J., Turlings, T.C.J., Guerin, P.M., Connétable, S., and Kuhlemeier, C. (2005). The composition and timing of flower odour emission by wild *Petunia axillaris* coincide with the antennal perception and nocturnal activity of the pollinator *Manduca sexta*. Planta *222*, 141–150.
38. Xu, S., Schlüter, P.M., Grossniklaus, U., and Schiestl, F.P. (2012). The genetic basis of pollinator adaptation in a sexually deceptive orchid. PLoS Genet. *8*, e1002889.
39. Muhlemann, J.K., Klempien, A., and Dudareva, N. (2014). Floral volatiles: from biosynthesis to function. Plant Cell Environ. *37*, 1936–1949.
40. Sheehan, H., Hermann, K., and Kuhlemeier, C. (2012). Color and scent: how single genes influence pollinator attraction. Cold Spring Harb. Symp. Quant. Biol. *77*, 117–133.
41. Riffell, J.A., Lei, H., Christensen, T.A., and Hildebrand, J.G. (2009). Characterization and coding of behaviorally significant odor mixtures. Curr. Biol. *19*, 335–340.
42. Riffell, J.A., Lei, H., Abrell, L., and Hildebrand, J.G. (2013). Neural basis of a pollinator's buffet: olfactory specialization and learning in *Manduca sexta*. Science *339*, 200–204.
43. Hermann, K., Klahre, U., Moser, M., Sheehan, H., Mandel, T., and Kuhlemeier, C. (2013). Tight genetic linkage of prezygotic barrier loci creates a multifunctional speciation island in *Petunia*. Curr. Biol. *23*, 873–877.
44. Verdonk, J.C., Haring, M.A., van Tunen, A.J., and Schuurink, R.C. (2005). *ODORANT1* regulates fragrance biosynthesis in *Petunia* flowers. Plant Cell *17*, 1612–1624.
45. Bombarely, A., Moser, M., Amrad, A., Bao, M., Bapaume, L., Barry, C.S., Bliek, M., Boersma, M.R., Borghi, L., Bruggmann, R., et al. (2016). Insight into the evolution of the Solanaceae from the parental genomes of *Petunia hybrida*. Nat. Plants *2*, 16074.
46. Verdonk, J.C., Ric de Vos, C.H., Verhoeven, H.A., Haring, M.A., van Tunen, A.J., and Schuurink, R.C. (2003). Regulation of floral scent production in *Petunia* revealed by targeted metabolomics. Phytochemistry *62*, 997–1008.
47. Klempien, A., Kaminaga, Y., Qualley, A., Nagegowda, D.A., Widhalm, J.R., Orlova, I., Shasany, A.K., Taguchi, G., Kish, C.M., Cooper, B.R., et al. (2012). Contribution of CoA ligases to benzenoid biosynthesis in *Petunia* flowers. Plant Cell *24*, 2015–2030.
48. Colquhoun, T.A., Marciniak, D.M., Wedde, A.E., Kim, J.Y., Schwieterman, M.L., Levin, L.A., Van Moerkercke, A., Schuurink, R.C., and Clark, D.G. (2012). A peroxisomally localized acyl-activating enzyme is required for

volatile benzenoid formation in a *Petunia*×*hybrida* cv. 'Mitchell Diploid' flower. J. Exp. Bot. *63*, 4821–4833.

49. Kapila, J., De Rycke, R., Van Montagu, M., and Angenon, G. (1997). An *Agrobacterium*-mediated transient gene expression system for intact leaves. Plant Sci. *122*, 101–108.
50. Segatto, A.L.A., Cazé, A.L.R., Turchetto, C., Klahre, U., Kuhlemeier, C., Bonatto, S.L., and Freitas, L.B. (2014). Nuclear and plastid markers reveal the persistence of genetic identity: a new perspective on the evolutionary history of *Petunia exserta*. Mol. Phylogenet. Evol. *70*, 504–512.
51. Turchetto, C., Segatto, A.L.A., Mäder, G., Rodrigues, D.M., Bonatto, S.L., and Freitas, L.B. (2016). High levels of genetic diversity and population structure in an endemic and rare species: implications for conservation. AoB Plants *8*, plw002.
52. Sheehan, H., Moser, M., Klahre, U., Esfeld, K., Dell'Olivo, A., Mandel, T., Metzger, S., Vandenbussche, M., Freitas, L., and Kuhlemeier, C. (2016). *MYB-FL* controls gain and loss of floral UV absorbance, a key trait affecting pollinator preference and reproductive isolation. Nat. Genet. *48*, 159–166.
53. Negre, F., Kish, C.M., Boatright, J., Underwood, B., Shibuya, K., Wagner, C., Clark, D.G., and Dudareva, N. (2003). Regulation of methylbenzoate emission after pollination in snapdragon and *Petunia* flowers. Plant Cell *15*, 2992–3006.
54. Boatright, J., Negre, F., Chen, X., Kish, C.M., Wood, B., Peel, G., Orlova, I., Gang, D., Rhodes, D., and Dudareva, N. (2004). Understanding in vivo benzenoid metabolism in *Petunia* petal tissue. Plant Physiol. *135*, 1993–2011.
55. Orlova, I., Marshall-Colón, A., Schnepp, J., Wood, B., Varbanova, M., Fridman, E., Blakeslee, J.J., Peer, W.A., Murphy, A.S., Rhodes, D., et al. (2006). Reduction of benzenoid synthesis in *Petunia* flowers reveals multiple pathways to benzoic acid and enhancement in auxin transport. Plant Cell *18*, 3458–3475.
56. Rockman, M.V. (2012). The QTN program and the alleles that matter for evolution: all that's gold does not glitter. Evolution *66*, 1–17.
57. Martin, A., and Orgogozo, V. (2013). The loci of repeated evolution: a catalog of genetic hotspots of phenotypic variation. Evolution *67*, 1235–1250.
58. Dittmar, E.L., Oakley, C.G., Conner, J.K., Gould, B.A., and Schemske, D.W. (2016). Factors influencing the effect size distribution of adaptive substitutions. Proc. Biol. Sci. *283*, 20153065.
59. Shields, V.D.C., and Hildebrand, J.G. (2000–2001). Responses of a population of antennal olfactory receptor cells in the female moth *Manduca sexta* to plant-associated volatile organic compounds. J. Comp. Physiol. A Neuroethol. Sens. Neural Behav. Physiol. *186*, 1135–1151.
60. Theis, N. (2006). Fragrance of Canada thistle (*Cirsium arvense*) attracts both floral herbivores and pollinators. J. Chem. Ecol. *32*, 917–927.
61. Yuan, Y.-W., Byers, K.J.R.P., and Bradshaw, H.D., Jr. (2013). The genetic control of flower-pollinator specificity. Curr. Opin. Plant Biol. *16*, 422–428.
62. Colquhoun, T.A., Kim, J.Y., Wedde, A.E., Levin, L.A., Schmitt, K.C., Schuurink, R.C., and Clark, D.G. (2011). *PhMYB4* fine-tunes the floral volatile signature of *Petunia*×*hybrida* through *PhC4H*. J. Exp. Bot. *62*, 1133–1143.
63. Spitzer-Rimon, B., Farhi, M., Albo, B., Cna'ani, A., Ben Zvi, M.M., Masci, T., Edelbaum, O., Yu, Y., Shklarman, E., Ovadis, M., and Vainstein, A. (2012). The R2R3-MYB-like regulatory factor EOBI, acting downstream of EOBII, regulates scent production by activating *ODO1* and structural scent-related genes in *Petunia*. Plant Cell *24*, 5089–5105.
64. Spitzer-Rimon, B., Marhevka, E., Barkai, O., Marton, I., Edelbaum, O., Masci, T., Prathapani, N.-K., Shklarman, E., Ovadis, M., and Vainstein, A. (2010). *EOBII*, a gene encoding a flower-specific regulator of phenylpropanoid volatiles' biosynthesis in *Petunia*. Plant Cell *22*, 1961–1976.
65. Sas, C., Müller, F., Kappel, C., Kent, T.V., Wright, S.I., Hilker, M., and Lenhard, M. (2016). Repeated inactivation of the first committed enzyme underlies the loss of benzaldehyde emission after the selfing transition in *Capsella*. Curr. Biol. Published online December 1, 2016. http://dx.doi.org/10.1016/j.cub.2016.10.026.
66. Shaipulah, N.F.M., Muhlemann, J.K., Woodworth, B.D., Van Moerkercke, A., Verdonk, J.C., Ramirez, A.A., Haring, M.A., Dudareva, N., and Schuurink, R.C. (2016). *CCoAOMT* down-regulation activates anthocyanin biosynthesis in *Petunia*. Plant Physiol. *170*, 717–731.

Current Biology, Volume *26*

Supplemental Information

Gain and Loss of Floral Scent Production through Changes in Structural Genes during Pollinator-Mediated Speciation

Avichai Amrad, Michel Moser, Therese Mandel, Michel de Vries, Robert C. Schuurink, Loreta Freitas, and Cris Kuhlemeier

Supplemental Experimental Procedures

Genotyping and marker association analyses

Genotyping of IL3-2 accessions for marker regression analysis was performed with the EOBII CAPS marker. Genotypic classes were not normally distributed (Shapiro-Wilk test), so tests for association of means with *EOBII* genotype were carried out using the Kruskal-Wallace one-way analysis of variance in R. Wild accessions were genotyped using Sanger sequencing with AA001 & AA004 primers (see Oligonucleotides Table below). Progeny of putative hybrid wild accessions were genotyped using a CNL1 CAPS marker based on a polymorphism located 18 bp upstream of the nonsense mutation. All details for CAPS markers can be found on http://www.botany.unibe.ch/deve/caps/index.html

Quantitative RT-PCR

Flower limb samples were collected one day after anthesis at 15:00, from three plants representing three biological replicates. RNA extraction was carried out using the RNeasy Plant Mini Kit (Qiagen). After extraction, RNA samples were treated with DNAse I (Sigma-Aldrich) to remove any remaining genomic DNA, and the quality of the RNA was subsequently measured on a 2100 Bioanalyzer (Agilent). Samples with RNA Integrity Numbers (RIN) less than 7.5 were discarded. First strand synthesis was performed using Transcriptor Universal cDNA Master (Roche) containing random hexamer primers, according to the manufacturer's recommendations. Quantitative RT-PCR experiments were performed using a LightCycler® 96 Real-Time PCR System (Roche) with FastStart Essential DNA Green Master qPCR Kit (Roche), according to the manufacturer's recommendations. Reactions were run in triplicates for each gene. Primers are given in the Oligonucleotides Table. Cycle of quantification (Cq) thresholds and normalization calculations were determined by the LightCycler® 480 Software (v.1.1.0.1320; Roche). Each biological replicate of each species was analyzed on a separate PCR plate and a single *P. axillaris* 15:00 sample from one biological replicate was included in each plate as a normalizer. Integration of data from biological replicates was conducted manually. Standard curves were performed to determine the PCR efficiency of each set of primers. No reverse-transcription controls were performed for each sample. Previously identified reference genes [S1] were tested for stability of expression across different *P. axillaris* and *P. exserta* samples and NormFinder [S2] was used to perform stability tests. *EF1α* and *SAND* were shown to be the most stable reference genes and were included for each sample.

RNA sequencing

For all experiments, three biological replicates were used for each genotype, and flower limb tissue was harvested one day after anthesis around 14:50 (at 15:00 is the transition from light to dark). For experiment one (comparisons of *P. axillaris*, *P. exserta* and IL3-2), biological replicates of *P. axillaris*, *P. exserta*, IL3-$2^{P.axi}$, IL3-2^{het} and IL3-$2^{P.exs}$ were sequenced. One of the *P. exserta* replicates was proven to be contaminated and was discarded from further analysis. For experiment two RNA was sequenced from *P. axillaris*, *P. inflata*, *P. exserta* and *P. axillaris* x *P. inflata* F1. RNA extraction was carried out using the RNeasy Plant Mini Kit (Qiagen).
RNA was sequenced in the Lausanne Genomic Technologies Facility (Lausanne, Switzerland). Quality of RNA was checked using a Fragment Analyzer (Advanced Analytical). For experiment one, RNA Quality Numbers (RQN) ranged from 5.9 to 8.8; for experiment two, RQN ranged from 6.6 to 9.8. Cluster generation was performed with the sequencing libraries using the Illumina TruSeq PE Cluster Kit (v.3). Samples from experiment one were paired-end sequenced and samples from experiment two single-end sequenced for 100 bp. Sequencing data were processed using the Illumina Pipeline Software v.1.82. For all samples, raw reads were checked for contamination by aligning them against rRNA sequences from *P. axillaris*, the *Escherichia coli* genome and the human transcriptome using bowtie2 (v.2.2.1) [S3]. Reads aligning to mentioned sequences were discarded. FastqMcf (v.1.1.2-686; http://code.google.com/p/ea-utils/wiki/FastqMcf) was used to remove Illumina adapter sequences and trim low quality regions. After trimming, reads shorter than 60 bp were discarded. These pre-processed reads were mapped against the draft reference genome of *P. axillaris* (v.1.6.2) [S4] using the SNP-tolerant and splice-aware aligner GSNAP (v.2015-06-12) [S5]. To allow for variation between reference and reads, the "–m" option was set to 0.04. Variant calling was carried out in GATK (v.3.4.0) [S6] according to GATK best practices for RNA-seq data. After duplicate marking and splitting reads with N in their CIGAR string, local realignment

around indels was undertaken, and base quality scores were recalibrated, using a set of high quality SNPs determined by an initial run of the GATK HaplotypeCaller. Those SNPs were used to determine genes being inside or outside of the introgressed region in IL3-2. Only exonic positions with maximal upstream distance of 100 bp from start codon and maximal downstream distance of 100 bp from stop codon were considered to detect allele-specific expression.

Differential expression analyses

Reads mapping to the genes of interest were counted using HTseq (v.0.6.1) in the union mode. Differential expression analysis was performed in R (http://www.R-project.org/) using DESeq2 (v.1.8.1) [S7] with the default parameters, including the Cook's distance treatment to remove outliers. Normalized read counts are presented in figures. Allelic coverage for variant positions was detected with ASEReadCounter implemented in GATK [S6,S8]. Analyses of allelic imbalance were conducted in R (http://www.R-project.org/) with the package MBASED (v.1.2.0) [S9]. Parameters of read count overdispersion were estimated with a custom R script provided by the author of the MBASED package (available on request).

Transient expression experiment

Transformation assays were done according to Van Moerkercke et.al 2011 [S10]. One-day-old flowers were syringe-infiltrated and two days later flower limbs were harvested. Tissue of four flowers were combined and homogenized in liquid nitrogen and transferred to a glass vial containing 2 ml of 1M NaCl 60°C. Immediately and following a short vortex samples were analyzed with PTR-MS for 30 cycles with an air inlet of approximately 20 L/h. Values were averaged and normalized to tissue weight before statistical analysis.

List of primers

Purpose	Gene/element	Primer name	Primer sequence (5' to 3')	Reference
Quantitative RT-PCR, reference gene	*SAND*	SAND-F	CTTACGACGAGTTCAGATGCC	[S1]
Quantitative RT-PCR, reference gene	*SAND*	SAND-R	TAAGTCCTCAACACGCATGC	[S1]
Quantitative RT-PCR, reference gene	*EF1α*	EF1α-F	CCTGGTCAAATTGGAAACGG	[S1]
Quantitative RT-PCR, reference gene	*EF1α*	EF1α-R	CAGATCGCCTGTCAATCTTGG	[S1]
Quantitative RT-PCR	*CNL*	qCNL_UF	GGGTACTTCAAGAATGACAAGGC	
Quantitative RT-PCR	*CNL*	qCNL_UR	CACCTAGGATGTGGCATGGC	
Genotyping by CNL1 sequencing	*CNL1*	AA001	TTCCGGCCAGTAAGTTATGG	
Genotyping by CNL1 sequencing	*CNL1*	AA004	TGTTGAAGTGTCTGACTGGTCA	
P. axillaris/P.exserta sequence	*CNL1*	cdsCNL_F	ATGGACGAGTTACCAAAATGTGG	
P. axillaris sequence	*CNL1*	cdsCNL_R	CTACAGACGAGCTGGCAAAT	
P. exserta sequence	*CNL1*	exsCNL1_R3	TCTGGGACGTTTGATTTGCA	
Gibson Assembly	*CNL1* cds	B470	CAACAAACAACATTACAATTTACTATTCTAGTCGAATGG ACGAGTTACCAAAATGTG	
Gibson Assembly	*P. axillaris CNL1* cds	B471	AGCTCAGACTAGGTGGATCTCTACAGACGAGCTGGCAA	
Gibson Assembly	*P. exserta CNL1* cds	B570	CTCAGACTAGGTGGATCTCTAGTAGTGACACATTGAATC TGG	
Gibson Assembly	35S promoter	B468	GGCCTCTTCGCTATTACGCCAGACTAGAGCCAAGCTGAT	
Gibson Assembly	35S promoter	B469	CATAGTTTGCTCCACATTTTGGTAACTCGTCCATTCGACT AGAATAGTAAATTGTAATGTTG	
Gibson Assembly	pGreenII vector	B477	GTAATGAAGGAGAAAACTCACCGAGGCAGTTCCATAGG ATGGCAAGATCCTG	
Gibson Assembly	pGreenII vector	B473	GCAAAGGAGATCAGCTTGGCTCTAGTCTGGCGTAATAG CGAAGAG	
Gibson Assembly	pGreenII vector	B472	AGATTCTTGATTTGCCAGCTCGTCTGTAGAGATCCACCT AGTCTGAG	
Gibson Assembly	pGreenII vector	B478	GTGATTTTGATGACGAGCGTAATGGCTGGCCTGTTGAAC AAG	
Gibson Assembly	pGreenII vector	B569	CCAGATTCAATGTGTCACTACTAGAGATCCACCTAGTCT GAG	

Supplemental References

1. Mallona, I., Lischewski, S., Weiss, J., Hause, B., and Egea-Cortines, M. (2010). Validation of reference genes for quantitative real-time PCR during leaf and flower development in Petunia hybrida. BMC Plant Biol. *10*, 4.

2. Andersen, C.L. (2004). Normalization of Real-Time Quantitative Reverse Transcription-PCR Data: a model-based variance estimation approach to identify genes suited for normalization, applied to bladder and colon cancer data sets. Cancer Res. *64*, 5245–5250.

3. Langmead, B., and Salzberg, S.L. (2012). Fast gapped-read alignment with Bowtie 2. Nat. Methods *9*, 357–359.

4. Bombarely, A., Moser, M., Amrad, A., Bao, M., Bapaume, L., Barry, C.S., Bliek, M., Boersma, M.R., Borghi, L., Bruggmann, R., et al. (2016). Insight into the evolution of the Solanaceae from the parental genomes of Petunia hybrida. Nat. Plants *2*, 16074.

5. Wu, T.D., and Nacu, S. (2010). Fast and SNP-tolerant detection of complex variants and splicing in short reads. Bioinformatics *26*, 873–881.

6. DePristo, M.A., Banks, E., Poplin, R., Garimella, K. V, Maguire, J.R., Hartl, C., Philippakis, A.A., del Angel, G., Rivas, M.A., Hanna, M., et al. (2011). A framework for variation discovery and genotyping using next-generation DNA sequencing data. Nat. Genet. *43*, 491–498.

7. Anders, S., Pyl, P.T., and Huber, W. (2015). HTSeq--a Python framework to work with high-throughput sequencing data. Bioinformatics *31*, 166–169.

8. Castel, S.E., Levy-Moonshine, A., Mohammadi, P., Banks, E., and Lappalainen, T. (2015). Tools and best practices for allelic expression analysis. bioRxiv, 016097.

9. Mayba, O., Gilbert, H.N., Liu, J., Haverty, P.M., Jhunjhunwala, S., Jiang, Z., Watanabe, C., and Zhang, Z. (2014). MBASED: allele-specific expression detection in cancer tissues and cell lines. Genome Biol. *15*, 405.

10. Van Moerkercke A., Haring M.A. and Schuurink R.C. (2011) The transcription factor EMISSION OF BENZENOIDS II activates the MYB *ODORANT1* promoter at a MYB binding site specific for fragrant petunias. Plant J. *67*, 917–928.